0026-895X/06/6901-27–36$20.00
MOLECULAR PHARMACOLOGY
Copyright © 2006 The American Society for Pharmacology and Experimental Therapeutics
Mol Pharmacol 69:27–36, 2006

Vol. 69, No. 1
15164/3068126
Printed in U.S.A.

Determinants of Zinc Potentiation on the α4 Subunit of Neuronal Nicotinic Receptors

Bernard Hsiao, Karla B. Mihalak, Sarah E. Repicky, Drew Everhart, Ana H. Mederos, Arun Malhotra, and Charles W. Luetje

Departments of Molecular & Cellular Pharmacology (B.H., K.B.M., S.E.R., D.E., A.H.M., C.W.L.) and Biochemistry & Molecular Biology (A.M.), Miller School of Medicine, University of Miami, Miami, Florida

Received June 9, 2005; accepted September 27, 2005

ABSTRACT

We have shown previously that the function of neuronal nicotinic acetylcholine receptors can be modulated by zinc. This modulation varies from potentiation to inhibition, depending on receptor subunit composition and zinc concentration, with the α4β2 and α4β4 receptors displaying the most dramatic potentiation. In this study, we used site-directed mutagenesis to identify glutamate 59 and histidine 162 on the rat α4 subunit as potential mediators of zinc potentiation. By modeling the extracellular domain of the receptor pentamer, we locate these residues to two subunit-subunit interfaces that alternate with the two acetylcholine-binding interfaces. Substitution of a cysteine at either position allows additional reduction of zinc potentiation upon treatment with the methanethiosulfonate reagents *N*-biotinoylaminoethyl methanethiosulfonate (MTSEA-biotin) and [2-(trimethylammonium)ethyl] methanethiosulfonate. Mutagenesis and methanethiosulfonate treatment are most effective at position 162, and the presence of zinc hinders the reaction of MTSEA-biotin with the substituted cysteine at this position, suggesting that α4His162 participates in forming a coordination site for zinc. Mutagenesis and methanethiosulfonate treatment are less effective at position 59, suggesting that whereas α4Glu59 may be near the zinc coordination site, it may not be participating in coordination of the zinc ion. It is noteworthy that the position of α4Glu59 within the neuronal nAChR is identical to that of a residue that lines the benzodiazepine-binding site on $GABA_A$ receptors. We suggest that the zinc potentiation sites on neuronal nAChRs are structurally and functionally similar to the benzodiazepine-binding sites on $GABA_A$ receptors.

Nicotinic acetylcholine receptors (nAChRs) belong to a family of neurotransmitter receptors that includes GABA-, glycine-, and serotonin-gated ion channels. Affinity labeling and mutagenesis studies suggest that agonist-binding sites on these pentameric receptors are located at interfaces between subunits (Corringer et al., 2000). On muscle nAChRs, agonist binding sites are located at the interfaces between the αγ and αδ subunit pairs, with the α subunits contributing a "principal component" of several amino acid sequence segments (A, B, and C) and the γ/δ subunits contributing a "complementary component" of several segments (D, E, and F) (Corringer et al., 2000). The structure of the acetylcholine binding protein (AChBP) confirms this model (Brejc et al., 2001; Smit et al., 2001; Celie et al., 2004). The AChBP homopentamer binds agonist at all five interfaces, with each AChBP monomer supplying the principal contribution to one binding site and the complementary contribution to another binding site. Some neuronal nAChRs are also homopentamers (α7) and form agonist-binding sites in a similar manner (Corringer et al., 1995). However, many neuronal nAChRs are heteromeric with some subunits making the principal contribution (α2-α4, α6) and others making the complementary contribution (β2, β4) (Corringer et al., 2000). For these receptors, the formation of an agonist-binding site at the interface between two dissimilar subunits, and the rotational symmetry revealed by the AChBP structure, limits the number of agonist binding sites to two. This raises an interesting

This work was supported by National Institutes of Health grants MH66038 and DA08102 (to C.W.L.) and GM069972 (to A.M.). A.M. was supported in part by award BM030 from the Florida Biomedical Research Foundation, and by American Heart Association, Florida/Puerto Rico Affiliate grant SDG-0130456B. B.H., K.B.M., D.E., and S.E.R. were supported in part by National Institutes of Health grant T32-HL07188. B.H. was supported in part by a PhRMA Foundation Medical Student Research Fellowship and is a Lois Pope LIFE Fellow.

B.H and K.B.M. contributed equally to this work.

Article, publication date, and citation information can be found at http://molpharm.aspetjournals.org.

doi:10.1124/mol.105.015164.

ABBREVIATIONS: nAChR, nicotinic acetylcholine receptor; AChBP, acetylcholine binding protein; SCAM, substituted cysteine accessibility method; MTSEA, *N*-biotinoylaminoethyl methanethiosulfonate; MTSET, [2-(trimethylammonium)ethyl] methanethiosulfonate; ACh, acetylcholine; MTS, methanethiosulfonate.

question. If only two interfaces are involved in binding agonist, what is the function of the other interfaces?

Ionic zinc is found in neurons throughout the brain, with highest concentrations in the cerebral cortex and limbic areas (Frederickson et al., 2000). Zn^{2+} is packaged in synaptic vesicles and, upon neuronal stimulation, is released in a calcium-dependent manner (Assaf and Chung, 1984; Howell et al., 1984). Estimates of extracellular [Zn^{2+}] during neuronal activity vary from 10~40 μM (Li et al., 2001) to 100~300 μM (Assaf and Chung, 1984; Vogt et al., 2000). Zn^{2+} modulates the function of neuronal nAChRs (Palma et al., 1998; Garcia-Colunga et al., 2001; Hsiao et al., 2001) and other ligand-gated ion channels (Huang, 1997), suggesting that Zn^{2+} is a modulator of synaptic activity. Indeed, synaptically released Zn^{2+} modulates synaptic activity in the hippocampus (Vogt et al., 2000; Ueno et al., 2002).

Some neuronal nAChRs, such as $\alpha4\beta2$ and $\alpha4\beta4$, are potentiated by micromolar Zn^{2+} and inhibited by millimolar Zn^{2+} (Hsiao et al., 2001). Others, such as $\alpha3\beta2$ (Hsiao et al., 2001) and $\alpha7$ (Palma et al., 1998), are only inhibited by Zn^{2+}. Results with chimeric receptor subunits, and the sensitivity of potentiation to diethylpyrocarbonate and changes in pH, indicate that extracellular histidines participate in forming the potentiating Zn^{2+} binding site(s) (Hsiao et al., 2001). In this study, we combined conventional mutagenesis, the substituted cysteine accessibility method (SCAM), and protein modeling to identify residues that are determinants of Zn^{2+} potentiation. Our results suggest that neuronal nAChRs bind ACh and Zn^{2+} at alternating subunit-subunit interfaces.

Materials and Methods

Molecular Biology. Mutations were introduced into rat neuronal nAChR subunits using the GeneEditor in vitro site-directed mutagenesis system (Promega, Madison, WI). All mutations were confirmed by sequencing. Capped cRNA encoding wild-type and mutant subunits was generated using mMessage mMachine kits (Ambion, Austin, TX).

Preparation of Oocytes and cRNA Injection. Oocytes were surgically removed from mature *Xenopus laevis* frogs (Nasco, Fort Atkinson, WI). The care and use of *X. laevis* frogs in this study were approved by the University of Miami Animal Research Committee and met the guidelines of the National Institutes of Health. Follicle cells were removed by treatment with Collagenase B (Roche Diagnostics, Indianapolis, IN) for 2 h at room temperature. Stage V oocytes were injected with 0.5 to 10 ng of each cRNA (at a molar ratio of 1:1) in 15 to 50 nl of water and incubated at 18°C in Barth's saline (88 mM NaCl, 1 mM KCl, 2.4 mM $NaHCO_3$, 0.3 mM $CaNO_3$, 0.41 mM $CaCl_2$, 0.82 mM $MgSO_4$, 15 mM HEPES, pH 7.6, and 100 μg/ml gentamicin) for 2 to 7 days.

Electrophysiology and Data Analysis. Current responses were measured under two-electrode voltage clamp, at a holding potential of −70 mV, using TEV-200 voltage clamp units (Dagan, Minneapolis, MN). Micropipettes were filled with 3 M KCl and had resistances of 0.3 to 2.0 MΩ. Current responses, filtered (8-pole, Bessel low pass) at 20 Hz (−3 db) and sampled at 100 Hz, were captured, stored, and analyzed using a Digidata 1322A (Molecular Devices, Sunnyvale, CA) in conjunction with either a Macintosh G3 computer running Axograph 4.6 software (Molecular Devices) or a Pentium III PC running pClamp 8 (Molecular Devices). Oocytes were perfused at room temperature (20–25°C), in a chamber constructed from Tygon tubing (inner diameter, 0.125 inches), with perfusion solution (115 mM NaCl, 1.8 mM $CaCl_2$, 2.5 mM KCl, 0.0001 mM atropine, and 10 mM HEPES, pH 7.2). Perfusion was continuous (except during MTSEA-biotin applications) at a rate of ~4 ml/min. ACh alone and in combination with Zn^{2+} was applied diluted in perfusion solution. Some experiments were conducted using an OpusXpress 6000A Parallel Oocyte Voltage Clamp system running OpusXpress 1.1 and Clampfit 9.1 software (Molecular Devices). In these experiments, all perfusion and application of ACh and Zn^{2+} was handled by the OpusXpress system. All Zn^{2+}-containing solutions were freshly prepared from a 1 M stock of $Zn(CH_3COO)_2$. In previous work, no difference was seen between the effects of $Zn(CH_3COO)_2$-and $ZnCl_2$-containing solutions (Hsiao et al., 2001). *X. laevis* oocytes express a Ca^{2+}-activated Cl^- channel that can contribute to whole-cell current responses when Ca^{2+} permeable channels, such as neuronal nAChRs, are activated. In previous work (Hsiao et al., 2001), we found that the extent of zinc potentiation did not vary across a range of holding potentials (−90 to −40 mV). Because the Cl^- channel current amplitude varies dramatically over this voltage range, our results led us to conclude that the Ca^{2+}-activated Cl^- channel does not underlie or affect measurement of zinc potentiation of neuronal nAChRs expressed in *X. laevis* oocytes. For this reason, we have chosen not to attempt to inhibit the Ca^{2+}-activated Cl^- channel.

Wild-type and mutant $\alpha4\beta4$ receptors displayed little or no desensitization in response to the low ACh concentrations used here, allowing measurement of Zn^{2+} potentiation as follows. Control current in response to ACh was determined from a 1-s average beginning 29 s after initiation of agonist application and compared with a 1-s average of baseline current immediately before ACh application. Current levels during Zn^{2+} coapplication were determined from a 1-s average beginning 29 s after initiation of Zn^{2+} application and compared with the control current. Potentiation of wild-type $\alpha4\beta4$ and all mutants (with one exception, see below) was determined with 1 μM ACh, which lies between the EC_1 and EC_6 for each receptor. We have previously found that the extent of zinc potentiation of wild-type $\alpha4\beta4$ does not vary across this portion of the ACh dose-response curve (Hsiao et al., 2001). For one mutant (α4-2E59C β4C75S), 1 μM ACh was the $EC_{0.2}$. For this receptor, we used 5 μM ACh (the EC_2) to test potentiation.

Wild-type and mutant $\alpha4\beta2$ receptors displayed substantial desensitization upon exposure to ACh, requiring measurement of potentiation or inhibition as described previously (Hsiao et al., 2001). In brief, the initial 30-s ACh response in the absence of Zn^{2+} was fit to a single exponential decay function. This fit was projected over the next 30 s during which both ACh and Zn^{2+} were coapplied. The degree of modulation was measured by taking a 1-s average 29 s after initiation of Zn^{2+} application and comparing it with a 1-s average of the projected response to ACh alone during the same time period. Thus, both Zn^{2+} and control values were taken 59 s after the initiation of the experiment. Potentiation of wild-type $\alpha4\beta2$ and all mutants was determined with 10 μM ACh, which lies between the EC_{14} and EC_{24} for each receptor. We have previously found that the extent of zinc potentiation of wild-type $\alpha4\beta2$ does not vary across this portion of the ACh dose-response curve (Hsiao et al., 2001). A similar extent of potentiation was also seen at the lower ACh concentration of 3 μM (the EC_3) (Hsiao et al., 2001).

In the SCAM experiments in Fig. 4, A to C, Zn^{2+} potentiation was measured before and after a 2-min incubation with 2 mM MTSEA-biotin (Toronto Research Chemicals, Inc., North York, ON, Canada). MTSEA-biotin was diluted from a dimethyl sulfoxide stock solution into perfusion solution immediately before application. The final DMSO concentration of 0.5% had no effect on ACh responses or zinc potentiation (data not shown). After the incubation, oocytes were rinsed for 5 min with perfusion solution before measuring Zn^{2+} potentiation. The high concentration of MTSEA-biotin and relatively long duration of the incubation were chosen to ensure saturation. Indeed, application of fresh reagent for a further 5-min incubation failed to cause any further loss of potentiation (data not shown). In some experiments, 1 mM MTSET was used.

In the SCAM reaction rate experiments in Fig. 4D, potentiation of the response of α4-2H162C β4C75S to 1 μM ACh by 100 μM Zn^{2+} was measured using our standard protocol. 1 μM MTSEA-biotin was

then applied for 5 s. The oocytes were then rinsed for 5 min and potentiation was measured again. This process was repeated and the cumulative exposure times used to determine the reaction rates in the presence and absence of 100 μM Zn^{2+}. The concentration of MTSEA-biotin (1 μM) that would yield a measurable reaction rate was determined empirically. Reaction rates were determined by fitting to the single exponential decay equation: $Y = Y_{max}e^{-kt}$, where Y is the potentiation at time t (in seconds), Y_{max} is the initial potentiation, and k is the pseudo–first-order rate constant. The second-order rate constant was obtained by dividing k by the concentration of MTSEA-biotin (Pascual and Karlin, 1998).

Both ACh and Zn^{2+} dose-response curves were fit according to the equation $I = I_{max}/[1 + (EC_{50}/X)^{nH}]$ where I represents the current response at a given concentration of ACh or Zn^{2+}, X; I_{max} is the maximal response; EC_{50} is the concentration of ACh or Zn^{2+} yielding a half-maximal response; n_H is the Hill coefficient. Zinc inhibition data (see *Results*) was fit according to the equation: $I = I_{max}/[1 + (X/IC_{50})^{nH}]$ where I represents the current response at a given metal concentration, X, I_{max} is the maximal current, IC_{50} is the concentrations of metal yielding half-maximal inhibition, and n_H is the Hill coefficient. Data presented in Fig. 3B was fit to a more complex equation that included both a potentiating and an inhibitory site: $I = I_{min} + (I_{max} - I_{min})\{[1/(1 + (EC_{50}/X)^{nH})] - [1/(1 + (IC_{50}/X)^{mH})]\}$, where I represents the current response at a given metal concentration, X, I_{min} is the minimal current, I_{max} is the maximal current, EC_{50} and IC_{50} are the concentration of metal yielding half-maximal potentiation and inhibition, respectively, and n_H and m_H are the Hill coefficients for potentiation and inhibition, respectively.

Data analysis was performed using Prism 3 software (GraphPad, San Diego, CA). Statistical significance was assessed using a two-tailed unpaired t test, or a one-way analysis of variance followed by the Dunnett's post-test, as appropriate.

Molecular Modeling. Sequence alignment of the amino-terminal extracellular region of the rat α4 and β4 neuronal nAChR subunits with the AChBP was performed using the Alignx module of Vector NTI 5 (InforMax, Inc., North Bethesda, MD). The alignments between the AChBP and α4 and β4 had identity values of 20.4 and 19.4%, respectively. Although the sequence identity between the AChBP monomer and amino-terminal extracellular domains of various nAChR subunits is relatively low, the presence of highly conserved ACh binding residues in the AChBP (Brejc et al., 2001), and the nicotinic pharmacology of the AChBP (Smit et al., 2001) suggests that homology modeling of neuronal nAChR extracellular domains using the AChBP structure is appropriate (Le Novere et al., 2002).

Three-dimensional models were constructed using the program Modeller 6 (Sali and Blundell, 1993) on a Silicon Graphics Indigo2 Extreme workstation. The script "model" was used with neuronal nAChR subunit/AChBP alignments. Disulfide bonds in the AChBP template structure were explicitly included during homology model refinement. The amino-terminal extracellular domain sequences of the α4 and β4 subunits were modeled using the AChBP pentamer structure (Brejc et al., 2001) (Protein Data Bank code 1I9B) to get initial coordinates for an $\alpha4\beta4$ pentamer (subunit ordering of $\alpha\beta\alpha\beta\beta$). Ten models were produced with energy refinement handled within the program. Conditions were optimized such that resulting structures exhibited energies in line with current published nicotinic receptor homology models (Le Novere et al., 2002; Everhart et al., 2003). The lowest energy structure was then inspected visually and with Procheck (Laskowski et al., 1993) for inappropriate stereochemistry (clashing side chains, disallowed torsion angles, etc.). In only one case did a residue require manual adjustment using the O software package (Jones et al., 1991). Further minimization was then carried out using the CNS software package (Brünger, 1998), with 20 cycles of conjugate gradient. The CNS minimized structure was then reanalyzed with Procheck to ensure stereochemical soundness. The images in Figs. 1B and 6 were produced using Ribbons (Carson, 1997). Coordinates for the final $\alpha4\beta4$ model may be obtained at http://chroma.med.miami.edu/pharm/faculty_Luetje.html.

Results

The effect of 100 μM Zn^{2+} on current responses induced by low concentrations of ACh varies from inhibition of $\alpha3\beta2$ receptors to greater than 5-fold potentiation of $\alpha4\beta4$ receptors, with the $\alpha3\beta4$ and $\alpha4\beta2$ receptors displaying intermediate levels of potentiation (Fig. 1A). The large difference in the effect of Zn^{2+} on $\alpha4\beta4$ and $\alpha3\beta2$ receptors suggested a strategy for identifying the site at which Zn^{2+} binds and potentiates neuronal nAChRs (i.e., mutagenesis of residues present in α4 and β4, but not in α3 and β2).

Amino acid residues that most commonly form Zn^{2+}-binding sites include histidines, free cysteines, aspartates, and glutamates (Glusker, 1991). Our previous work indicated the involvement of extracellular histidine residues (Hsiao et al., 2001), so we used site-directed mutagenesis to test the role of the seven histidine residues unique to the extracellular portions of α4 and β4. We also examined the two unique extracellular free cysteine residues. Our screen included five residues within the amino-terminal extracellular domain of α4 (His2, His61, His104, His109, His162), two residues within this region of β4 (Cys75, His157), one residue within the carboxyl-terminal extracellular portion of α4 (Cys594), and one residue within the carboxyl-terminal extracellular portion of β4 (His469). At some positions, the residue was changed to the residue present at that position in α3 or β2, as appropriate. For α4His2, α4His104, and β4Cys75, the residues present in α3 and β2 might also be Zn^{2+}-coordinating (glutamate, aspartate, and aspartate, respectively). Thus, in addition to testing α4H2E and α4H104D mutants, we also tested the alanine mutants α4H2A and α4H104A. For β4Cys75, we tested a serine mutant. To test the role of α4Cys594, we used a naturally occurring splice variant (α4-2) that lacks this C-terminal cysteine (Goldman et al., 1987). The positions of these residues within an alignment of α3, α4, β2, and β4 are shown in Fig. 1C. To visualize the positions of these residues within the receptor structure, we generated a homology model of the extracellular domain of the $(\alpha4)_2(\beta4)_3$ pentamer using the AChBP (Brejc et al., 2001) as a template structure (see *Materials and Methods*). Many of these residues are located at the non–ACh-binding subunit-subunit interfaces within the pentamer (Fig. 1B).

We used the $\alpha4\beta4$ receptor as our primary target to allow analysis of α4 and β4 residues in the same receptor. The $\alpha4\beta4$ receptor is also convenient because it displays the greatest degree of zinc potentiation, expresses well in oocytes, and shows little or no desensitization in response to low ACh concentrations. The role of critical residues in α4 was also confirmed with $\alpha4\beta2$ (see below), a major nAChR subtype in the mammalian central nervous system (Corringer et al., 2000). Mutant α4 and β4 subunits were coexpressed in *X. laevis* oocytes with wild-type β4 or α4 subunits, respectively. ACh dose-response curves, constructed for each mutant receptor, showed that the mutations had little or no effect on ACh sensitivity (Table 1). We used 100 μM Zn^{2+} to test the effect of each mutation because 100 μM Zn^{2+} lies at the peak of the biphasic potentiation-inhibition curve for $\alpha4\beta4$ (Hsiao et al., 2001). Thus, reductions in maximal potentiation or shifts in the curve would be detected. Compared with wild-type $\alpha4\beta4$ receptors, some mutant receptors (such as α4H162Gβ4) displayed reduced potentiation by 100 μM Zn^{2+} (45 $\pm$ 4% of wild-type), whereas others (such as

$\alpha4\beta4$C75S) displayed potentiation similar to that of wild-type $\alpha4\beta4$ (Fig. 2A). In addition to α4H162G, the α4H61N, and β4H469Y mutations also caused significant decreases in potentiation by 100 μM Zn^{2+} (Fig. 2B, Table 2). The $\alpha4$-2$\beta4$ receptor (which lacks the C-terminal cysteine) displayed an increase in potentiation, suggesting potential involvement in the allosteric pathway. However, because we are focused on identifying the zinc potentiation site, we chose not to pursue this possibility. In our model of the $\alpha4\beta4$ extracellular domain, the side chains of β4Asp195 and α4Glu59 are near the side chain of α4His162 (Fig. 1B). Because Asp195 is conserved in both the $\beta2$ and $\beta4$ subunits, we substituted an alanine at this position. We also prepared a α4E59A mutant. The α4E59A$\beta4$ receptor displayed significantly reduced potentiation by 100 μM Zn^{2+}, whereas the $\alpha4\beta4$D195A receptor did not differ from wild-type $\alpha4\beta4$ (Fig. 2B). The results of this mutagenesis screen identify α4Glu59, α4His61, α4His162, and β4His469 as candidates for involvement in forming the zinc potentiation site.

In Fig. 3A, we examined the effects of a range of zinc concentrations on wild-type and mutant $\alpha4\beta4$ receptors. The α4E59A, α4H61N, α4H162G, and β4H469Y mutations each reduced maximal potentiation by Zn^{2+}, but none of the mutations increased the EC_{50} for zinc potentiation, as might be expected if the mutations were damaging a zinc-binding site (Table 2). However, a simple rightward shift in the zinc dose-response curve could be expected only if zinc potentiation were occurring in isolation. We have previously shown that zinc both potentiates and inhibits these receptors at separate sites. At and above 300 μM Zn^{2+}, receptor inhibition of the $\alpha4\beta4$ receptor becomes apparent, leading to a distinctly biphasic Zn^{2+} dose-response curve (Hsiao et al., 2001). If the mutations were causing damage to the potentiation site but leaving the inhibition site intact, a rightward shift in the potentiation curve could be obscured.

To investigate this issue in more detail, we examined the effects of a wider range of Zn^{2+} concentrations on the α4H162G$\beta4$ mutant (Fig. 3B). Obtaining accurate values from fitting biphasic zinc dose-response data to a two-site equation is difficult because of the close proximity of potentiating and inhibiting phases (Hsiao et al., 2001). However, in this earlier study, we found that diethylpyrocarbonate treatment eliminates potentiation, without affecting inhibition, of the $\alpha4\beta4$ receptor. We fit these data to a single-site inhibition equation to obtain an IC_{50} for Zn^{2+} inhibition of 362 $\pm$ 70 μM (see *Materials and Methods*). We then fit the biphasic zinc dose-response data for wild-type $\alpha4\beta4$ in our earlier study to a two-site equation (see *Materials and Methods*) using this IC_{50} value as a constant. This allowed us to estimate parameters for zinc potentiation of the wild type $\alpha4\beta4$ receptor (EC_{50} = 110 $\pm$ 33 μM, n_H = 0.96 $\pm$ 0.04, maximal potentiation = 1400 $\pm$ 250%). The EC_{50} value is 4-fold greater and the maximal potentiation value 2-fold greater than what we obtain when we fit the potentiating phase of the data to a single site equation. This suggests that the inhibiting phase does indeed partially obscure the poten-

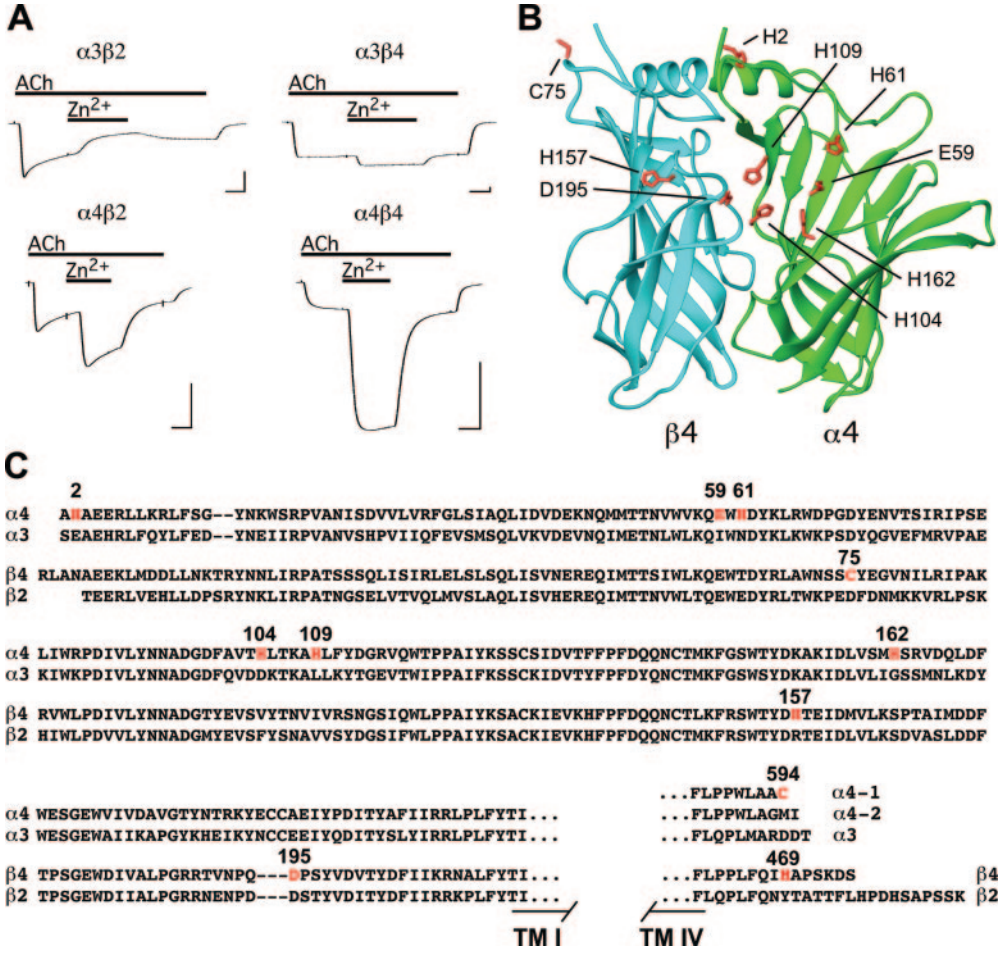

Fig. 1. A, the effect of Zn^{2+} varies with receptor subunit composition. ACh induced current responses of oocytes expressing the indicated neuronal nAChRs before, during, and after coapplication of 100 μM Zn^{2+}. ACh concentrations for each receptor are $\alpha3\beta2$ = 4 μM (EC_{10}), $\alpha3\beta4$ = 17 μM (EC_2), $\alpha4\beta2$ = 10 μM (EC_{14}), $\alpha4\beta4$ = 1 μM (EC_2). Scale bars, 250 nA, 10 s. B, two subunits, $\beta4$ (blue) and $\alpha4$ (green), taken from our homology model of the pentameric $\alpha4\beta4$ receptor extracellular domain are shown. Residues tested in this study are indicated in red. α4Cys594 and β4His469 are not shown because they are not within the homology model. C, alignment of the N-terminal extracellular domains (preceding transmembrane I) of $\alpha4$, $\alpha3$, $\beta4$, and $\beta2$, and the C-terminal extracellular tails (after transmembrane IV) of $\alpha4$–1, $\alpha4$–2, $\alpha3$, $\beta4$, and $\beta2$. Residues tested in this study are indicated in red.

tiation phase. Because zinc inhibition occurs at a separate class of site (Hsiao et al., 2001), it is unlikely to be affected by mutations at the zinc potentiation site. This allows us to use the inhibition parameters obtained from fitting the postdiethylpyrocarbonate treatment wild-type $\alpha4\beta4$ receptor when fitting the data obtained for the $\alpha4H162G\beta4$ mutant. If we also assume that maximal potentiation is not changing, we find that upon fitting to a two-site equation, the EC_{50} for zinc potentiation of the $\alpha4H162G\beta4$ mutant is greater (267 ± 7 μM) than the value for wild-type $\alpha4\beta4$. This analysis suggests, but does not prove, that the $\alpha4H162G\beta4$ receptor is indeed less sensitive to zinc potentiation than wild-type $\alpha4\beta4$. To prove this conclusively using dose-response analysis, we would need to be able to examine potentiation in the absence of inhibition. However, we have been unable to eliminate, or even damage, the inhibition of nAChRs by zinc (Hsiao et al., 2001). None of the mutations we have examined reduces inhibition by high concentrations of zinc (data not shown). Thus, we turned to other approaches to provide additional information about the role of candidate residues in forming the zinc potentiation site.

First, we examined the effect of double mutant combinations, reasoning that simultaneous mutation of two residues involved in mediating zinc potentiation should yield an effect greater than with either single mutation. Because the $\alpha4H162G$ mutant displayed the greatest loss of Zn^{2+} potentiation, we used this receptor as a point of reference. Each of the other three mutations was examined as a double mutant with $\alpha4H162G$. The $\alpha4H61N$ and $\beta4H469Y$ mutations failed to alter potentiation of the $\alpha4H162G$ $\beta4$ receptor. Potentiation of these double mutants by 100 μM Zn^{2+} was 107 ± 7 and 99 ± 7% of the potentiation of the $\alpha4H162G$ single mutant, respectively. This result suggests that these residues might not play important roles in mediating Zn^{2+} potentiation. In contrast, receptors formed by the double mutant $\alpha4E59A,H162G$ displayed significantly decreased potentiation compared with the potentiation of $\alpha4H162G$ (81 ± 5% of the single mutant potentiation, $p < 0.05$, $n = 13$). It is noteworthy that potentiation was not completely eliminated. Receptors formed by the $\alpha4E59A,H162G$ double mutant retained a modest ability to be potentiated by Zn^{2+} (36% of wild-type; see *Discussion*).

As an alternative approach to testing the role of candidate residues in forming a zinc potentiation site, we turned to SCAM (Karlin and Akabas, 1998). In SCAM analysis, a cysteine is placed at the position of interest and function is then measured before and after reaction with a methanethiosulfonate (MTS) reagent. Although free cysteines can participate in coordination of Zn^{2+}, they often do not substitute effectively for other coordinating residues (Paoletti et al., 2000), probably because of the stringent spatial requirements for the relevant atoms (S, N, and O) to be able to coordinate the zinc ion. The result of our double-mutant experiments (see above) suggest that even if a substituted cysteine failed to directly participate in Zn^{2+} coordination (thus constituting a single mutant), the functional damage to the site would be partial. A further reduction of Zn^{2+} potentiation after reaction with an MTS reagent would then suggest a physical proximity to the zinc ion and would strengthen the case for direct coordination. As the MTS reagent for most of our experiments, we used MTSEA-biotin, a large, relatively membrane impermeant MTS reagent that has been used to characterize various sites on $GABA_A$ recep-

TABLE 1
ACh sensitivity of wild-type and mutant neuronal nAChRs
EC_{50} and n_H values were determined by fitting to a Hill equation (see *Materials and Methods*). Values are the mean ± S.E.M. of data from three to nine oocytes.

Receptor	EC_{50}	n_H
	μM	
WT $\alpha4\beta4$	19 ± 4	1.3 ± 0.3
$\alpha4H2E$ $\beta4$	21 ± 7	0.9 ± 0.3
$\alpha4H2A$ $\beta4$	31 ± 11	1.1 ± 0.4
$\alpha4E59A$ $\beta4$	39 ± 10	0.8 ± 0.2
$\alpha4H61N$ $\beta4$	19 ± 4	1.2 ± 0.3
$\alpha4H104D$ $\beta4$	23 ± 5	1.0 ± 0.2
$\alpha4H104A$ $\beta4$	43 ± 10	1.3 ± 0.3
$\alpha4H109L$ $\beta4$	17 ± 5	1.4 ± 0.6
$\alpha4H162G$ $\beta4$	15 ± 2	1.6 ± 0.3
$\alpha4$-2 $\beta4$	32 ± 6	1.1 ± 0.2
$\alpha4$ $\beta4C75S$	17 ± 3	1.5 ± 0.4
$\alpha4$ $\beta4H157R$	17 ± 3	1.2 ± 0.3
$\alpha4$ $\beta4D195A$	25 ± 3	0.9 ± 0.1
$\alpha4$ $\beta4H469Y$	14 ± 3	1.2 ± 0.2
$\alpha4E59A$, $H162G$ $\beta4$	25 ± 4	1.2 ± 0.2
$\alpha4H61N$, $H162G$ $\beta4$	14 ± 8	1.0 ± 0.7
$\alpha4H162G$ $\beta4H469Y$	21 ± 4	1.0 ± 0.1
$\alpha4$-2 $\beta4C75S$ (pseudo-WT)	34 ± 12	0.9 ± 0.3
$\alpha4$-2$E59C$ $\beta4C75S$	39 ± 7	1.7 ± 0.5
$\alpha4$-2$H61C$ $\beta4C75S$	23 ± 3	1.2 ± 0.2
$\alpha4$-2$H162C$ $\beta4C75S$	21 ± 3	1.1 ± 0.1
WT $\alpha4\beta2$	33 ± 8	1.5 ± 0.4
$\alpha4E59A$ $\beta2$	42 ± 21	0.8 ± 0.2
$\alpha4H162G$ $\beta2$	27 ± 7	1.3 ± 0.3

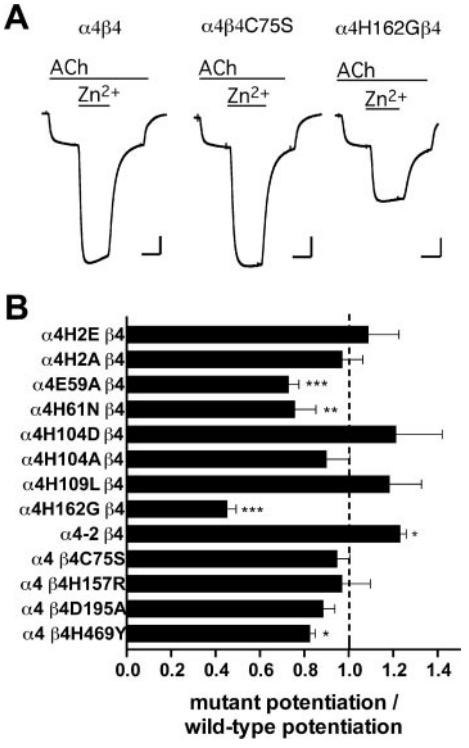

Fig. 2. Mutation analysis to identify candidate Zn^{2+} coordinating residues. A, current responses of oocytes expressing wild-type $\alpha4\beta4$ (left), $\alpha4\beta4C75S$ (center), or $\alpha4H162G\beta4$ (right) to 1 μM ACh before, during, and after coapplication of 100 μM Zn^{2+}. Scale bars: $\alpha4\beta4$ and $\alpha4H162G\beta4$, 200 nA and 20 s; $\alpha4\beta4C75S$, 100 nA and 20 s. B, potentiation of mutant receptors by 100 μM Zn^{2+}. Results are presented as the ratio of mutant receptor potentiation to the potentiation of wild-type receptor in the same batch of oocytes (mean ± S.E.M., n = 3–14). The ACh concentration for all receptors is 1 μM. Significant differences in Zn^{2+} potentiation compared with wild-type $\alpha4\beta4$ are indicated (***, $p < 0.001$; **, $p < 0.01$; *, $p < 0.05$).

tors (Teissere and Czajkowski, 2001; Wagner and Czajkowski, 2001). To avoid the potential for confounding effects of the MTS reagent acting at other free cysteines, the α4-2 β4C75S mutant receptor, which lacks extracellular free cysteine residues, was used as a "pseudo–wild-type" background (Karlin and Akabas, 1998) in which to test each cysteine mutant. This pseudo–wild-type receptor displayed ACh sensitivity and Zn^{2+} potentiation similar to that of true wild-type α4β4 and was unaffected by MTSEA-biotin treatment (Tables 1 and 2; Fig. 4, A and C).

We prepared E59C, H61C, and H162C mutants, each within the context of the pseudo–wild-type receptor. Each mutation resulted in significantly reduced Zn^{2+} potentiation (61 ± 5, 63 ± 9, and 77 ± 2% of pseudo–wild-type potentiation, respectively), similar to what was seen with the E59A, H61N, and H162G mutations. MTSEA-biotin treatment (2 mM, 2 min) had no significant effect on the ACh responses of any of the mutant receptors (data not shown). MTSEA-biotin also had no effect on Zn^{2+} potentiation of the α4H61C receptor (Fig. 4C), again suggesting that α4His61 may not play an important role in mediating Zn^{2+} potentiation. In contrast, MTSEA-biotin treatment significantly reduced potentiation of the α4E59C and α4H162C receptors, suggesting that α4Glu59 and α4His162 are located at or near the Zn^{2+}-binding site (Fig. 4, B and C). However, as was the case for the double mutant, these MTSEA-biotin treated mutant receptors retained some ability to be potentiated by Zn^{2+}. In Fig. 4, we used 1 μM ACh to test potentiation of the pseudo–wild-type receptor, as well as the α4H61C and α4H162C receptors. However, we used the equipotent concentration of 5 μM ACh to test potentiation of the α4E59C (see *Materials and Methods*). We also tested the ability of MTSEA-biotin to reduce zinc potentiation of the α4E59C using 1 μM ACh, finding post-treatment potentiation to be 76 ± 4% of pretreatment potentiation ($p < 0.05$, $n = 6$). Zinc potentiation could also be reduced by MTSET application (1 mM, 2 min). Although the trimethylammonium ethyl group deposited by MTSET is substantially smaller than the biotinylaminoethyl group deposited by MTSEA-biotin, it does have a positive charge that would be likely to interfere with Zn^{2+} binding. Post-treatment potentiation of α4-2H162C β4C75S by 100 μM Zn^{2+} was 71 ± 3% of pretreatment potentiation ($n = 6$, $p < 0.001$) and for α4-2E59C β4C75S, the value was 83 ± 3% of pretreatment potentiation ($n = 3$, $p < 0.05$). The effects of MTSEA-biotin and MTSET on zinc potentiation of the α4E59C mutant were substantially less than the effects on the α4H162C mutant. This may be because substitution of a cysteine for α4Glu59 had a greater effect on zinc potentiation than did substitution of α4His162 (61 ± 5 and 77 ± 2% remaining potentiation, respectively). Thus, there is less remaining potentiation to be affected by the MTS reagent. However, it is also possible that although α4Glu59 may be near the site of zinc binding, it might not be directly participating in coordination of the zinc ion.

SCAM can also be used to obtain information about the relative accessibility of a site under different conditions (Karlin and Akabas, 1998). By alternating short exposures to low concentrations of MTS reagent with functional measurements, a reaction rate (and thus a relative measure of accessibility) can be determined (Pascual and Karlin, 1998). In Fig. 4D, we use this method to examine the relative accessibility for MTSEA-biotin at position 162 of α4 in the presence and absence of Zn^{2+}. Oocytes expressing α4-2H162C β4C75S were exposed to 1 μM MTSEA-biotin in 5-s increments. After each application, the oocytes were rinsed, and the extent of potentiation by 100 μM Zn^{2+} was determined. The decline in Zn^{2+} potentiation upon repeated exposure to MTSEA-biotin was then fit to an exponential decay function. In the absence of Zn^{2+}, the half-time of the reaction was 8.7 s, yielding a rate of 79,000 ± 14,000 $M^{-1}s^{-1}$. In the presence of 100 μM Zn^{2+}, the halftime of the reaction was 21.3 s, yielding a rate of 32,000 ± 10,000 $M^{-1}s^{-1}$. Despite the change in reaction rate,

TABLE 2

Zinc potentiation of wild-type and mutant neuronal nAChRs

Data is presented as the ratio of potentiation of the mutant receptors to potentiation of wild-type receptors expressed in the same batch of oocytes (mean ± S.E.M., $n = 3$–13). For α4β4, Zn^{2+} concentration was 100 μM. For α4β2, Zn^{2+} concentration was 50 μM. The overall value for potentiation of wild-type α4β4 was 579 ± 13% of ACh alone ($n = 48$). The overall value for potentiation of wild-type α4β2 was 241 ± 14% of ACh alone ($n = 15$). Fit maximum potentiation, EC_{50}, and Hill coefficient (n_H) were determined by fitting the data in Fig. 6 to a Hill equation (mean ± S.E.M., $n = 4$–6).

Receptor	Potentiation (Mutant/WT)	Fit Maximum Potentiation	EC_{50}	n_H
		% of ACh	*μM*	
WT α4β4	1.00	660 ± 53	26 ± 6	1.8 ± 0.5
α4H2E β4	1.08 ± 0.14			
α4H2A β4	0.97 ± 0.09			
α4E59A β4	0.73 ± 0.05***	454 ± 23***	17 ± 2	1.6 ± 0.4
α4H61N β4	0.75 ± 0.10*	444 ± 32***	23 ± 5	1.5 ± 0.4
α4H104D β4	1.21 ± 0.21			
α4H104A β4	0.90 ± 0.11			
α4H109L β4	1.18 ± 0.15			
α4H162G β4	0.45 ± 0.04***	301 ± 19***	18 ± 4	1.5 ± 0.3
α4-2 β4	1.23 ± 0.03*			
α4 β4C75S	0.94 ± 0.06			
α4 β4H157R	0.97 ± 0.13			
α4 β4D195A	0.88 ± 0.05			
α4 β4H469Y	0.82 ± 0.03*	451 ± 16***	21 ± 2	1.4 ± 0.2
α4-2 β4C75S (pseudo-WT)	0.93 ± 0.06			
WT α4β2	1.00			
α4E59A β2	0.58 ± 0.13†††			
α4H162G β2	0.38 ± 0.05†††			

* $P < 0.05$, significant difference in potentiation compared with wild-type α4β4.
** $P < 0.01$, significant difference in potentiation compared with wild-type α4β4.
*** $P < 0.001$, significant difference in potentiation compared with wild-type α4β4.
††† $P < 0.001$, significant difference in potentiation compared with wild-type α4β2.

the extent of the effect was the same in the presence and absence of Zn^{2+} (the fit plateau was 0.69 ± 0.05 and 0.65 ± 0.02, respectively). The significant decrease in reaction rate ($p < 0.01$) indicates that the site is less accessible to MTSEA-biotin when Zn^{2+} is present and suggests that Zn^{2+} is competing with MTSEA-biotin for occupation of the site.

In addition to potentiation of the ACh response, zinc potentiates the response of neuronal nAChRs to nicotine. Potentiation of $\alpha4\beta4$ by coapplication of 100 μM Zn^{2+} with 1 μM nicotine was 444 ± 43% of the response to nicotine alone. The α4H162G and α4E59A mutant receptors each displayed significantly reduced potentiation by 100 μM Zn^{2+} (50 ± 5% of wild-type $\alpha4\beta4$, $p < 0.05$, and 88 ± 4% of wild-type $\alpha4\beta4$, $p < 0.01$, respectively).

We also examined the effect of mutating α4His162 and α4Glu59 in a different receptor subunit context: $\alpha4\beta2$ (Fig. 5). The $\alpha4\beta2$ is a major nAChR subtype in the central nervous system (Corringer et al., 2000). The effect of zinc on $\alpha4\beta2$ receptors was substantial, with a maximum potentiation of approximately 2.5-fold achieved at 50 μM Zn^{2+} (Figs. 1A and 5A, and see Hsiao et al., 2001). The α4E59A and α4H162G mutations were each able to significantly reduce the extent of potentiation by 50 μM Zn^{2+} (Fig. 5B).

Discussion

We have identified α4Glu59 and α4His162 as determinants of Zn^{2+} potentiation on rat neuronal nAChRs. The positions of these residues within our receptor model are shown in Fig. 6. A strong case can be made for direct coordination of the zinc ion by α4His162. Mutation of this residue results in a large loss of zinc potentiation; MTSEA-biotin has a substantial effect when a cysteine is at this position, and zinc can slow the reaction of MTSEA-biotin with a cysteine at this position. Although the side chain on α4Glu59 is close enough to the side chain of α4His162 (in Fig. 1B, the ϵN of

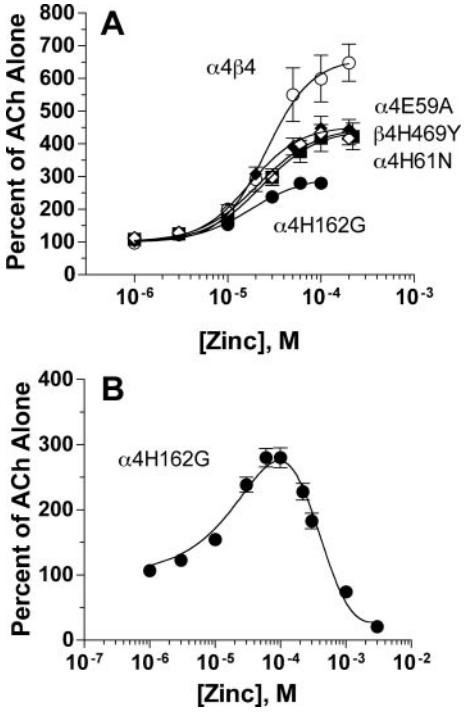

Fig. 3. A, the effects of a range of zinc concentrations on wild-type $\alpha4\beta4$ (○), α4E59A$\beta4$ (♦), α4H61N$\beta4$ (■), α4H162G$\beta4$ (●), and $\alpha4\beta4$H469Y (◇) receptors are plotted as a percentage of the response to 1 μM ACh alone. Values are the mean ± S.E.M. from 3 to 6 oocytes and are fit to a Hill equation (see *Materials and Methods*). B, the potentiating and inhibiting phases of the action of zinc on α4H162G$\beta4$ receptors is shown. Values are the mean ± S.E.M. from three oocytes and are fit to a dual-site Hill equation (see *Results* for an explanation).

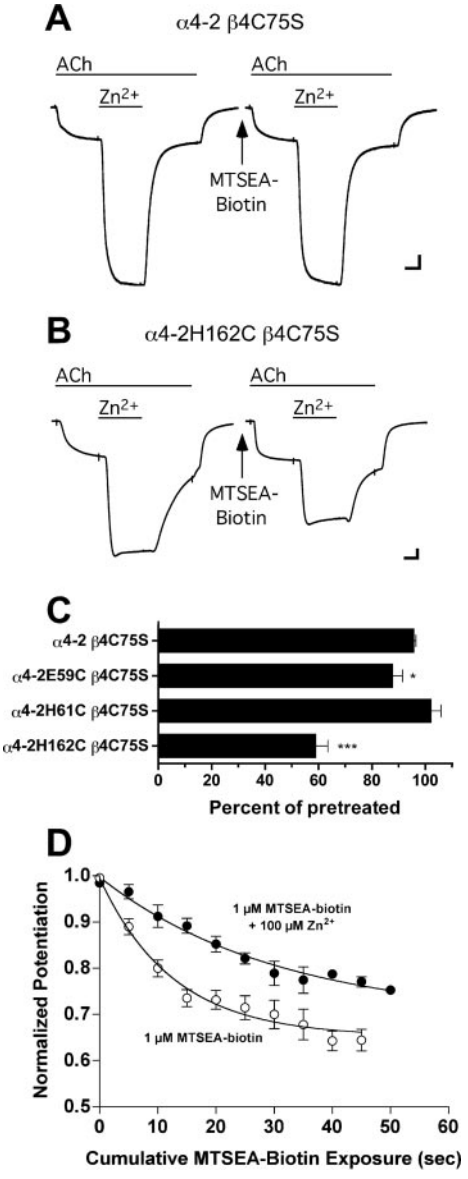

Fig. 4. SCAM analysis at the Zn^{2+} potentiation site. A, potentiation of the ACh (1 μM) response of an $\alpha4$-2β4C75S (pseudo–wild-type) expressing oocyte by 100 μM Zn^{2+} before and after a 2-min incubation with 2 mM MTSEA-biotin (scale, 100 nA, 10 s). B, potentiation of the ACh (1 μM) response of an α4-2H162C,β4C75S-expressing oocyte by 100 μM Zn^{2+} before and after a 2-min incubation with 2 mM MTSEA-biotin (scale, 100 nA, 10 s). C, potentiation of the α4E59C, α4H61C, and α4H162C mutants (each expressed within the context of the pseudo–wild-type receptor, $\alpha4$-2β4C75S) by 100 μM Zn^{2+}, measured after a 2-min incubation with 2 mM MTSEA-biotin, is plotted as a percentage of pretreatment potentiation (mean ± S.E.M., n = 3–5). Significant differences from pretreated: *, $p < 0.05$; ***, $p < 0.001$. D, reaction rates for MTSEA-biotin at $\alpha4$-2H162C β4C75S in the presence and absence of 100 μM Zn^{2+}. Potentiation of the response to 1 μM ACh was measured before and after successive 5-s applications of 1 μM MTSEA-biotin. Results are presented as the ratio of post-treatment potentiation to the initial, pretreatment potentiation. Values are the mean ± S.E.M. from three to six oocytes and are fit to an exponential decay equation (see *Materials and Methods*).

His162 is 5.6 Å from the nearest carboxyl oxygen in Glu59) for a role in coordination to be plausible (Harding, 2001), the effects of mutation and MTSEA-biotin treatment are substantially less than what is seen at position 162. Thus, although α4His162 is likely to be participating in direct coordination of the zinc ion, α4Glu59 may only be near the zinc potentiation site without actually participating in zinc coordination.

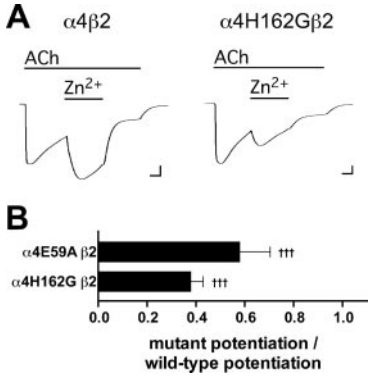

Fig. 5. Mutation of α4Glu59 or α4His162 decreases zinc potentiation of α4β2 receptors. A, current responses of oocytes expressing wild-type α4β2 (left) or α4H162Gβ2 (right) to 10 μM ACh before, during, and after coapplication of 50 μM Zn^{2+}. Scale bars are 2 μA and 10 s. B, potentiation of mutant receptors by 50 μM Zn^{2+}. Results are presented as the ratio of mutant receptor potentiation to the potentiation of wild type receptor in the same batch of oocytes (mean ± S.E.M., n = 13–15). Significant differences in Zn^{2+} potentiation compared with wild-type α4β2 are indicated (†††, $p < 0.001$).

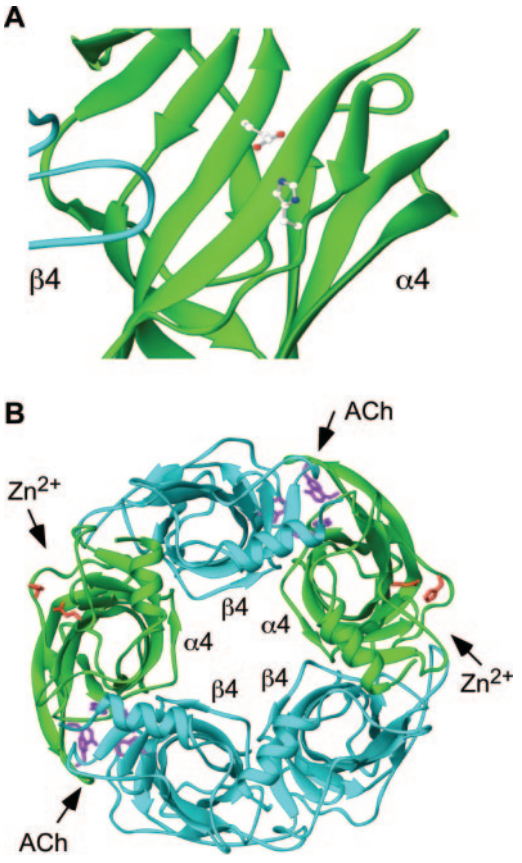

Fig. 6. Neuronal nAChRs bind zinc and ACh at alternating subunit-subunit interfaces. A, zinc-binding residues at a β4-α4 interface. Residues α4Glu59 and α4His162 are shown. B, the extracellular domain of the α4β4 pentamer is shown viewed from above. α4 subunits are green, β4 subunits are blue. Side chains of several residues that are conserved features of ACh binding sites (α4-Tyr93, Trp149, Tyr190, Tyr197, and β4-Trp59) are shown in purple. Side chains of α4Glu59 and α4His162 are shown in red.

The Location of Zinc Potentiation Sites on Neuronal nAChRs. The positions of α4His162 and α4Glu59 within the receptor and the involvement of both α and β subunits in mediating Zn^{2+} potentiation (Hsiao et al., 2001) suggest that neuronal nAChRs bind Zn^{2+} at subunit-subunit interfaces that alternate with ACh-binding interfaces. This depends on our decision to model the receptor with a subunit arrangement of αβαββ. Whether the fifth subunit is β or α is irrelevant. In either case, the receptor would have two ACh-binding and two zinc-binding interfaces. More important is the arrangement of the first four subunits in an alternating αβαβ pattern. This arrangement seems to be required. The subunits of the AChBP are arranged in a rotationally symmetric manner, with each subunit supplying a principal face to one ACh binding site and a complementary face to another ACh binding site (Brejc et al., 2001; Celie et al., 2004). In heteromeric neuronal nAChRs, the principal residues are only present on the α subunit, whereas the complementary residues are only present on the β subunit (Corringer et al., 2000). Thus, both α and β subunits are required to form an ACh binding site. Regardless of whether the α/β stoichiometry is 2:3 or 3:2, only two nonadjacent interfaces will form ACh binding sites. An additional two nonadjacent interfaces would form Zn^{2+}-binding sites.

Neuronal nAChRs also form as homopentamers of the α7 subunit (Corringer et al., 2000). The α7 subunit lacks both His162 and Glu59 (Le Novere and Changeux, 2001), and α7 homopentamers are thought to bind ACh at all five interfaces (Corringer et al., 2000). As would be expected, α7 homomers are not potentiated by Zn^{2+} (Palma et al., 1998). A novel Zn^{2+}-activated channel (ZAC) has been reported (Davies et al., 2003). This homomeric receptor is structurally homologous to nAChRs. Whereas ZAC subunits have a histidine in a position similar to that of α4His162, no aspartates or glutamates are located near the position analogous to α4Glu59. It is unclear whether the ZAC binds Zn^{2+} at a site similar to the potentiation site we have identified on neuronal nAChRs.

We have identified at least one residue (α4His162) as part of a pair of identical Zn^{2+} potentiation sites on neuronal nAChRs. Because Zn^{2+}-binding sites can have four, five, or six coordination points (Glusker, 1991), additional residues remain to be identified. These receptors may also possess a second class of Zn^{2+} potentiation site. In our single-mutation experiments, only partial losses of potentiation were observed. This was not unexpected. However, even the double mutant α4E59A,H162G retained a modest ability to be potentiated by Zn^{2+} application (approximately one third of wild-type potentiation). In our SCAM experiments, we also did not completely eliminate potentiation. This contrasts with the complete elimination of potentiation upon diethypyrocarbonate treatment (Hsiao et al., 2001). Thus, neuronal nAChRs might possess at least three distinct classes of Zn^{2+} binding site: a major potentiation site accounting for roughly two thirds of the potentiation (identified here), a minor potentiation site accounting for roughly one third of the potentiation, and an inhibitory site. Glutamate, GABA and glycine receptors also possess multiple classes of Zn^{2+} modulatory

sites (Paoletti et al., 2000; Laube et al., 2002; Hosie et al., 2003).

Zinc Potentiation Sites Have Structural Similarities to ACh Binding Sites. We compared the zinc potentiation site with other binding sites on Cys-loop receptors. The ACh binding site on nAChRs has been extensively characterized (Corringer et al., 2000). Glu59 is located within the "D-loop" region of α4. In an ACh-binding interface, the D-loop is supplied by the γ, δ, or ϵ subunits of muscle nAChRs or the β subunits of neuronal nAChRs and contributes a critical tryptophan residue to the binding site, as well as several determinants of pharmacological diversity (Corringer et al., 2000; Celie et al., 2004). His162 is located within the "F-loop" region of α4. At ACh binding interfaces, this region is also supplied by the "non-α" subunits of muscle and neuronal nAChRs and contains determinants of pharmacological diversity (Corringer et al., 2000). Thus, the Zn^{2+}-binding site that we have identified has structural similarity to the ACh binding site.

Zinc Potentiation Sites Are Not Related to Calcium Potentiation Sites on Neuronal nAChRs. Neuronal nAChRs are also potentiated by extracellular Ca^{2+} (Mulle et al., 1992; Vernino et al., 1992). Critical glutamate residues mediating Ca^{2+} potentiation have been identified on α7 (Galzi et al., 1996). These residues are highly conserved among neuronal nAChRs and correspond to α4Glu45/β4Glu49 (located between β strands 1 and 2) and α4Glu175/β4Glu179 (located just before β strand 9). Both putative Ca^{2+} binding sites are located at the bottom (near the membrane) of the receptor structure shown in Fig. 1B, away from the Zn^{2+} potentiation site we have identified. In addition, Ca^{2+} potentiation of α4β4 is unaffected by the α4H162G and α4E59A mutations (data not shown). Thus, Zn^{2+} and Ca^{2+} act at separate sites on neuronal nAChRs.

Zinc Potentiation Sites Are Not Related to Zinc Binding Sites of Other Ligand-Gated Ion Channels. Other Cys-loop receptors also possess Zn^{2+}-binding sites. On the glycine receptor α1 subunit, Asp80 participates in a Zn^{2+}-potentiation site at subunit-subunit interfaces near the top (distal from the cell surface) of the receptor extracellular domain, whereas His107, His109, and Thr112 participate in an inhibitory site that faces into the vestibule (Laube et al., 2002). The Zn^{2+} site that we have identified on neuronal nAChRs is not structurally comparable with either of these sites. $GABA_A$ receptors also possess multiple Zn^{2+}-binding sites. For clarity, it is important to remember that $GABA_A$ receptor β subunits are equivalent to neuronal nAChR α subunits, whereas $GABA_A$ receptor α subunits are equivalent to neuronal nAChR β subunits. Thus, whereas neuronal nAChRs bind ACh at α-β interfaces, GABA receptors bind GABA at β-α interfaces (Smith and Olsen, 1995). In the α1β3 $GABA_A$ receptor, α1Glu137, α1His141 and β3Glu182 participate in a Zn^{2+}-binding inhibitory site located at α-β interfaces (non-GABA binding interfaces) near the bottom (proximal to the cell surface) of the receptor extracellular domain (Hosie et al., 2003). A separate class of Zn^{2+}-binding inhibitory site is located within the ion channel. The Zn^{2+}-potentiation site we have identified on neuronal nAChRs is not structurally comparable with either of these Zn^{2+}-binding sites on $GABA_A$ receptors. Glutamate-gated ion channels also possess zinc-binding sites, which have been characterized in detail (Paoletti et al., 2000). However, these receptors are structurally unrelated to nAChRs, precluding a comparison with the Zn^{2+}-potentiation site on neuronal nAChRs.

Zinc Potentiation Sites Are Analogous to the Benzodiazepine-Binding Site on $GABA_A$ Receptors. The most interesting comparison is with the binding site for benzodiazepines on $GABA_A$ receptors. Whereas GABA binds at β-α interfaces, incorporation of a γ subunit allows benzodiazepines to bind at the α-γ interface (Smith and Olsen, 1995). A series of residues on the γ2 subunit (Tyr58, Phe77, Ala79, and Thr81) have been identified as components of the benzodiazepine-binding site (Kucken et al., 2000, 2003; Teissere and Czajkowski, 2001). Examination of aligned amino acid sequences (Le Novere and Changeux, 2001) and a model of the α1β2γ2 $GABA_A$ receptor extracellular domain (Kucken et al., 2003) reveals that the benzodiazepine-binding site residue γ2Thr81 (Teissere and Czajkowski, 2001) is in a location identical to that of α4Glu59. Although α4Glu59 may not directly coordinate zinc, it is close to the zinc potentiation site on neuronal nAChRs. This suggests that the binding of agonists and modulators at alternating subunit-subunit interfaces is a general property of heteromeric Cys-loop receptors. The similar location of the zinc potentiation sites on neuronal nAChRs and the benzodiazepine binding site on $GABA_A$ receptors, as well as the similar modulatory function of both sites, leads us to suggest that the Zn^{2+} potentiation sites on neuronal nAChRs are structurally and functionally similar to the benzodiazepine binding site on $GABA_A$ receptors. This identifies the Zn^{2+} potentiation site on neuronal nAChRs as a promising target for future drug development.

References

Assaf SY and Chung S-H (1984) Release of endogenous Zn^{2+} from brain tissue during activity. *Nature (Lond)* **308:**734–736.

Brejc K, van Dijk WJ, Klaassen RV, Schuurmans M, van der Oost J, Smit AB, and Sixma TK (2001) Crystal structure of an ACh-binding protein reveals the ligand-binding domain of nicotinic receptors. *Nature (Lond)* **411:**269–276.

Brünger AT (1998) Crystallography & NMR System: a new software suite for macromolecular structure determination. *Acta Crystallogr Sect D* **54:**905–921.

Carson M (1997) Ribbons. *Methods Enzymol* **277:**493–505.

Celie PHN, van Rossum-Fikkert SE, van Dijk WJ, Brejc K, Smit AB, and Sixma TK (2004) Nicotine and caramylcholine binding to nicotinic acetylcholine receptors as studied in AChBP crystal structures. *Neuron* **41:**907–914.

Corringer PJ, Galzi JL, Eisele JL, Bertrand S, Changeux JP, and Bertrand D (1995) Identification of a new component of the agonist binding site of the nicotinic alpha 7 homooligomeric receptor. *J Biol Chem* **270:**11749–11752.

Corringer PJ, Le Novere N, and Changeux JP (2000) Nicotinic receptors at the amino acid level. *Annu Rev Pharmacol Toxicol* **40:**431–458.

Davies PA, Wang W, Hales TG, and Kirkness EF (2003) A novel class of ligand-gated ion channel is activated by Zn^{2+}. *J Biol Chem* **278:**712–717.

Everhart D, Reiller E, Mirzoian A, McIntosh JM, Malhotra A, and Luetje CW (2003) Identification of residues that confer α-conotoxin PnIA sensitivity on the α3 subunit of neuronal nicotinic acetylcholine receptors. *J Pharmacol Exp Ther* **306:**664–670.

Frederickson CJ, Suh SW, Silva D, Frederickson CJ, and Thompson RB (2000) Importance of zinc in the central nervous system: the zinc-containing neuron. *J Nutrition* **130:**1471S–1483S.

Galzi JL, Bertrand S, Corringer PJ, Changeux JP, and Bertrand D (1996) Identification of calcium binding sites that regulate potentiation of a neuronal nicotinic acetylcholine receptor. *EMBO (Eur Mol Biol Organ) J* **15:**5824–5832.

Garcia-Colunga J, Gonzalez-Herrera M, and Miledi R (2001) Modulation of alpha2beta4 neuronal nicotinic acetylcholine receptors by zinc. *Neuroreport* **12:**147–150.

Glusker JP (1991) Structural aspects of metal liganding to functional groups in proteins. *Adv Protein Chem* **42:**1–76.

Goldman D, Deneris E, Luyten W, Kochhar A, Patrick J, and Heinemann S (1987) Members of a nicotinic acetylcholine receptors gene family are expressed in different regions of the mammalian central nervous system. *Cell* **48:**965–973.

Harding MM (2001) Geometry of metal-ligand interactions in proteins. *Acta Crystallogr Sect D* **57:**401–411.

Hosie AM, Dunne EL, Harvey RJ, and Smart TG (2003) Zinc-mediated inhibition of $GABA_A$ receptors: discrete binding sites underlie subtype specificity. *Nat Neurosci* **6:**362–369.

Howell GA, Welch MG, and Frederickson CJ (1984) Stimulation-induced uptake and release of zinc in hippocampal slices. *Nature (Lond)* **308:**736–738.

Hsiao B, Dweck D, and Luetje CW (2001) Subunit-dependent modulation of neuronal nicotinic receptors by zinc. *J Neurosci* **21:**1848–1856.

Huang EP (1997) Metal ions and synaptic transmission: think zinc. *Proc Natl Acad Sci USA* **94:**13386–13387.
Jones TA, Zou J-Y, Cowan S, and Kjeldgaard M (1991) Improved methods for building protein models in electron density maps and the location of errors in these models. *Acta Crystallogr Sect A* **47:**110–119.
Karlin A and Akabas MH (1998) Substituted-cysteine accessibility method. *Methods Enzymol* **293:**123–145.
Kucken AM, Teissere JA, Seffinga-Clark J, Wagner DA, and Czajkowski C (2003) Structural requirements for imidazobenzodiazepine binding to $GABA_A$ receptors. *Mol Pharmacol* **63:**289–296.
Kucken AM, Wagner DA, Ward PR, Teissere JA, Boileau AJ, and Czajkowski C (2000) Identification of benzodiazepine binding residues in the γ2 subunit of the γ-aminobutyric $acid_A$ receptor. *Mol Pharmacol* **57:**932–939.
Laskowski RA, MacArthur MW, Moss DS, and Thornton JM (1993) PROCHECK: a program to check the stereochemical quality of protein structures. *J Appl Crystallogr* **26:**283–291.
Laube B, Maksay G, Schemm R, and Betz H (2002) Modulation of glycine receptor function: a novel approach for therapeutic intervention at inhibitory synapses. *Trends Pharmacol Sci* **23:**519–527.
Le Novere N and Changeux J-P (2001) LGICdb: the ligand-gated ion channel database. *Nucleic Acids Res* **29:**294–295.
Le Novere N, Grutter T, and Changeux J-P (2002) Models of the extracellular domain of the nicotinic receptors and of agonist- and Ca^{2+}-binding sites. *Proc Natl Acad Sci USA* **99:**3210–3215.
Li Y, Hough CJ, Suh SW, Sarvey JM, and Frederickson CJ (2001) Rapid translocation of Zn^{2+} from presynaptic terminals into postsynaptic hippocampal neurons after physiological stimulation. *J Neurophysiol* **86:**2597–2604.
Mulle C, Choquet D, Korn H, and Changeux JP (1992) Calcium influx through nicotinic receptors in rat central neurons: its relevance to cellular regulation. *Neuron* **8:**937–945.
Palma E, Maggi L, Miledi R, and Eusebi F (1998) Effects of Zn^{2+} on wild and mutant neuronal α7 nicotinic receptors. *Proc Natl Acad Sci USA* **95:**10246–10250.
Paoletti P, Perin-Dureau F, Fayyazuddin A, Le Goff A, Callebaut I, and Neyton J (2000) Molecular organization of a zinc binding N-terminal modulatory domain in a NMDA receptor subunit. *Neuron* **28:**911–925.
Pascual JM and Karlin A (1998) State-dependent accessibility and electrostatic potential in the channel of the acetylcholine receptor. *J Gen Physiol* **111:**717–739.
Sali A and Blundell TL (1993) Comparative protein modeling by satisfaction of spatial restraints. *J Mol Biol* **234:**779–815.
Smit AB, Syed NI, Schaap D, van Minnen J, Klumperman J, Kits KS, Lodder H, van der Schors RC, van Elk R, Sorgedrager B, et al. (2001) A glia-derived acetylcholine-binding protein that modulates synaptic transmission. *Nature (Lond)* **411:**261–268.
Smith GB and Olsen RW (1995) Functional domains of $GABA_A$ receptors. *Trends Pharmacol Sci* **16:**162–168.
Teissere JA and Czajkowski C (2001) A β-strand in the γ2 subunit lines the benzodiazepine binding site of the $GABA_A$ receptor: structural rearrangements detected during channel gating. *J Neurosci* **21:**4977–4986.
Ueno S, Tsukamoto M, Hirano T, Kikuchi K, Yamada MK, Nishiyama N, Nagano T, Matsuki N, and Ikegaya Y (2002) Mossy fiber Zn^{2+} spillover modulates heterosynaptic *N*-methyl-D-aspartate receptor activity in hippocampal CA3 circuits. *J Cell Biol* **158:**215–220.
Vernino S, Amador M, Luetje CW, Patrick J, and Dani JA (1992) Calcium modulation and high calcium permeability of neuronal nicotinic acetylcholine receptors. *Neuron* **8:**127–134.
Vogt K, Mellor J, Tong G, and Nicoll R (2000) The actions of synaptically released zinc in hippocampal mossy fiber synapses. *Neuron* **26:**187–196.
Wagner DA and Czajkowski C (2001) Structure and dynamics of the GABA binding pocket: a narrowing cleft that constricts during activation. *J Neurosci* **21:**67–74.

Address correspondence to: Dr. Charles W. Luetje, Molecular and Cellular Pharmacology, R-189, University of Miami, P.O. Box 016189, Miami, FL 33101. E-mail: cluetje@chroma.med.miami.edu